Characterization of $(P^+L_x)L_y$ Ion Molecule Clusters of First-Row Hydrides

Xabier Lopez,* Jesus M. Ugalde, and Fernando P. Cossío

Contribution from Kimika Fakultatea, Euskal Herriko Unibertsitatea, P.K. 1072, 20080 Donostia, Euskadi, Spain

Received July 10, 1995. Revised Manuscript Received January 9, 1996[⊗]

Abstract: Ab initio calculations of phosphorus ionic clusters of the type $PL^+\cdot L$, $PL_2^+\cdot L$, PL_3^+, and PL_4^+, with L = NH_3, OH_2, and FH, in both triplet and singlet states have been carried out, in order to determine their geometries and binding energies. The nature of the binding has also been extensively studied by means of both the topological analysis of the total electron charge density and the natural bond orbital analysis. When the ligand is bound as a second ligation shell through a formal hydrogen bond, significant cooperative effects between the two ligand shells have been detected. Substantial covalency is found for these hydrogen bonds, along with the weakening of the hydride bond with the inner ligand and the reinforcing of the bond between the inner ligand and the phosphorus. These processes are greatly favored for the singlet state of the phosphorus, and for the case of ammonia and water ligands, conversion reactions leading to $PXH_{n-1}\cdot XH_{n+1}^+$ complexes are observed. It has been found that the maximum number of ligands bound to $(^3P)P^+$ is two, whereas that maximum is ligand dependent in the case of $(^1D)P^+$, with two for NH_3, three for OH_2, and four for FH. We have also observed that soft ligands present a sharp decrease in successive binding energies to phosphorus, whereas hard ligands show smoother variations. Finally, for most cases, the addition of the new ligand as a second ligation shell is favored with respect to the direct addition to the phosphorus, since cooperative effects make more efficient the donation of electronic charge to the phosphorus ion.

1. Introduction

The study of the formation and properties of small ionic clusters has been a topic of major interest during recent years.[1,2] Apart from intrinsic interest in understanding the forces between ions and neutral molecules, clusters have been the focus of a great deal of attention since they can be considered as a bridge between the gas and condensed phases, and in this sense, the understanding of the stability of the clusters and their chemistry can shed light on the differences between the reactivities of these phases. Also, clusters are relevant for phenomena such as nucleation, development of surfaces, solvation, catalysis, acid−base chemistry, combustion, and atmospheric processes.

Both theoretical[3−22] and experimental techniques[23−45] have been employed in the determination of various properties of ionic clusters. One of the major impetuses for these studies is to quantify the potential of interaction between ions and neutral molecules, i.e., the well depth or binding energy. It has been observed that alkali ions[3,4,9,14,24,25,33] exhibit an electrostatic binding mechanism, and the trends in successive binding energies can be well explained by solely electrostatic arguments. Quite interestingly, clusters of transition metal ions[5−8,26−28,35,44] also require the consideration of their electronic structure for a reliable explanation of their binding trends. On the other hand, clusters of open electronic shell ions[29−31] such as Sr^+, Pb^+, or Bi^+ (which is isovalent, $6s^26p^2$, to P^+, $3s^23p^2$) show some degree of covalency or chemical bonding at small cluster sizes. At larger cluster sizes, the electrostatic binding is regained, so for these ions, the binding in the first clusterification step is significantly different from that of sequential steps. In general, the nature of both the ion and ligand has a great influence for small clusters; however, as the clusters grow, similar binding energies are found, irrespective of the nature of the ligand or of the ion. It is also noteworthy that for some ions there exists a critical cluster size[1] (magic numbers) for which binding energies show a sharp decrease.

Therefore, there exists a large variety of structures and binding forces within the ion−molecule clusters. They depend not only on the nature of both the ion and the ligand but also on the size

[⊗] Abstract published in *Advance ACS Abstracts,* March 1, 1996.

(1) Castleman, A. W., Jr.; Keesee, R. G. *Chem. Rev.* **1986**, *86*, 589.
(2) Keesee, R. G.; Castleman, A. W., Jr. *J. Phys. Chem. Ref. Data* **1986**, *15*, 1011.
(3) Spears, K. G. *J. Chem. Phys.* **1972**, *57*, 1850.
(4) Woodin, R. L.; Houle, F. A.; Goddard, W. A., III. *Chem. Phys.* **1976**, *14*, 461.
(5) Rosi, M.; Bauschlicher, C. W., Jr. *J. Chem. Phys.* **1989**, *90*, 7264.
(6) Rosi, M.; Bauschlicher, C. W., Jr. *J. Chem. Phys.* **1990**, *92*, 1876.
(7) Bauschlicher, C. W., Jr.; Langhoff, S. R.; Partridge, H.; Rice, J. E.; Komornicki, A. *J. Chem. Phys.* **1991**, *95*, 5142.
(8) Langhoff, S. R.; Bauschlicher, C. W., Jr.; Partridge, H.; Sodupe, M. *J. Phys. Chem.* **1991**, *95*, 10677.
(9) Bauschlicher, C. W., Jr.; Langhoff, S. R.; Partridge, H. *J. Chem. Phys.* **1991**, *95*, 4142.
(10) Bauschlicher, C. W., Jr.; Partridge, H. *J. Phys. Chem.* **1991**, *95*, 9694.
(11) Bauschlicher, C. W., Jr.; Sodupe, M.; Partridge, H. *J. Chem. Phys.* **1992**, *96*, 4453.
(12) Kochanski, E. *J. Am. Chem. Soc.* **1985**, *107*, 7869.
(13) Kochanski, E.; Constantin, E. *J. Chem. Phys.* **1987**, *87*, 1661.
(14) Magnusson, E. *J. Phys. Chem.* **1994**, *98*, 12558.
(15) Magnusson, E.; Moriarty, N. *J. Comput. Chem.* **1993**, *14*, 961.
(16) Sannigrahi, A. B.; Nandi, P. K.; Schleyer, P. v. R. *J. Am. Chem. Soc.* **1994**, *116*, 7225.
(17) Deakyne, C. A. *J. Phys. Chem.* **1986**, *90*, 6625.
(18) Hashimoto, K.; Yoda, N.; Iwata, S. *Chem. Phys.* **1987**, *116*, 193.
(19) Hashimoto, K.; Iwata, S. *J. Phys. Chem.* **1989**, *93*, 2165.
(20) Hashimoto, K.; Yoda, N.; Osamura, Y.; Iwata, S. *J. Am. Chem. Soc.* **1990**, *112*, 7189.
(21) Watanabe, H.; Iwata, S.; Hashimoto, K.; Misaizu, F.; Fuke, K. *J. Am. Chem. Soc.* **1995**, *117*, 755.
(22) Bock, C. W.; Kaufman, A.; Glusker, J. P. *Inorg. Chem.* **1994**, *33*, 419.
(23) Kar, T.; Yoda, N.; Scheiner, S. *J. Am. Chem. Soc.* **1995**, *117*, 1344.
(24) Glendenning, E. D.; Feller, D. *J. Phys. Chem.* **1995**, *99*, 3060.
(25) Kebarle, P.; Dzidic, I. *J. Phys. Chem.* **1970**, *74*, 1466.
(26) Magnera, T. F.; David, D. E.; Michl, J. *J. Am. Chem. Soc.* **1989**, *111*, 4100−4101.
(27) Marinelli, P. J.; Squires, R. R. *J. Am. Chem. Soc.* **1989**, *111*, 4101−4103.
(28) Magnera, T. F.; David, D. E.; Stulik, D.; Orth, R. G.; Jonkman, H. T.; Michl, J. *J. Am. Chem. Soc.* **1989**, *111*, 5036−5043.
(29) Tang, I. N.; Castleman, A. W., Jr. *J. Chem. Phys.* **1972**, *57*, 3638.
(30) Tang, I. N.; Castleman, A. W., Jr. *J. Chem. Phys.* **1974**, *60*, 3981.
(31) Tang, I. N.; Lian, M. S.; Castleman, A. W., Jr. *J. Chem. Phys.* **1976**, *65*, 4022.
(32) Tang, I. N.; Castleman, A. W., Jr. *J. Chem. Phys.* **1975**, *62*, 4576.

0002-7863/96/1518-2718$12.00/0

of the cluster. In fact, differences in reactivity with the cluster size have been observed[39] along with changes in the nature of the central ion with the successive clusterification processes. These phenomena, collectively referred to as *conversion reactions*,[1] yield neutrals and ions different from the initial molecular entities.

In a series of papers,[46−49] we have theoretically characterized phosphorus ion clusters of the type PL_n^+ with $n = 1,2$ and L = NH_3, OH_2, FH, PH_3, SH_2, and ClH for both triplet and singlet spin states of the phosphorus ion. We found that one-ligand phosphorus clusters in both of the spin states satisfy the Pearson's hard and soft acid and base (HSAB) principle.[50−52] In this sense, as it corresponds to soft acids, phosphorus prefers to bind soft bases, for which the electronic interactions are more enhanced, rather than hard bases, which favor the electrostatic type of binding mechanism. Regarding to two ligand complexes, the same was found to be true for the singlets; however, for triplets, binding energies were found to fall down and covalency to lose importance.

In this paper, we get further into the understanding of phosphorus clusters by the addition of a ligand on the second ligation shell and by the study of larger cluster sizes. We have focused our attention on first-row hydrides. In this sense, we have characterized singlet and triplet $PL^+\cdot L$ complexes (i.e., one ligand bound to phosphorus and another one to this ligand) with L = NH_3, OH_2, and FH. These are the simplest systems with a ligand in a second ligation shell, and their detailed study can shed light on the cooperative effects among various ligation shells. We have also tried to determine the maximum number of ligands in the first ligation shell for the P^+ ion and its dependency upon the spin state of P^+ and the nature of the ligand. For this purpose, we have studied three-ligand complexes, with the third ligand bound either to the phosphorus (PL_3^+ complexes) or to one of the inner ligands ($PL_2^+\cdot L$ complexes), and four-ligand complexes. We have employed the G2* methodology for the study of $PL^+\cdot L$ complexes (namely, G2 methodology[53−55] applied at MP2/6-31G(d,p) geometries). On the other hand, the characterization of bigger clusters has been accomplished using density functional theory,[56a] namely, its B3LYP[56b] form. Topological analysis of the electronic charge density[57] and the natural bond orbital (NBO) analysis[58] have also been carried out in order to understand the binding features of such clusters.

We hope that these studies will contribute to clarify several features of phosphorus ion cluster's stability and reactivity, such as the effect of the second ligation shell, maximum number of ligands in the first ligation shell, the lowering of binding energies as the cluster grows and its relationship with the nature of the P−X bond, and last but not least, possible conversion reactions within a given cluster.

2. Methods

2.1. $PL^+\cdot L$ Complexes. To characterize these species, we have followed the G1 and G2 methodologies[53−55] with slight modifications. First, we have used a larger basis set in the optimizations, namely, the 6-31G(d,p) instead of the proposed[59] 6-31G(d), since inclusion of polarization on the hydrogens has been claimed to be essential to describe hydrogen bonds.[60] So, all structures were optimized at the MP2/6-31G(d,p) level of theory, and the resultant geometries can be found in Figure 1. Analytical frequencies at the stationary points were calculated at the same level of theory, and all of them were confirmed to be positive. We have used these frequencies to evaluate the corresponding zero-point vibrational energy (ZPVE) corrections to the total energy. Apart from this, G1 and G2 methodologies have been followed closely to evaluate the energies. All these calculations have been performed using the GAUSSIAN92/DFT suite of programs.[61]

Base level energies corrected by ZPVE and G1* and G2* energies can be found in Table 1 of the supporting information. Using the G2* energies we have evaluated the binding energy D_0 as

$$(D_0)_{PL_{n^+}} = E_{PL_{n^+}} - (E_{PL_{n-1^+}} + E_L) \qquad (1)$$

These energies can be found in Table 1 along with the relative energies of two-ligand complexes. It should be mentioned that for PL_{n-1^+} and L we have used the G2 energies calculated in our previous studies.[48] Notice that for the $PXH_{n-1^+}\cdot XH_{n+1^+}$ complexes, the binding energies are calculated with respect to the dissociation products $PXH_{n-1^+} + XH_{n+1^+}$.

(33) Castleman, A. W., Jr.; Holland, P. M.; Lindsay, D. M.; Peterson, K. I. *J. Am. Chem. Soc.* **1978**, *100*, 6039.
(34) Castleman, A. W., Jr. *Chem. Phys. Lett.* **1978**, *53*, 560.
(35) Holland, P. M.; Castleman, A. W., Jr. *J. Chem. Phys.* **1982**, *76*, 4195.
(36) Peterson, K. I.; Mark, T. D.; Keesee, R. G.; Castleman, A. W., Jr. *J. Phys. Chem.* **1984**, *88*, 2880.
(37) Gleim, K. L.; Guo, B. C.; Keesee, R. G.; Castleman, A. W., Jr. *J. Phys. Chem.* **1989**, *93*, 6805.
(38) Keesee, R. G.; Castleman, A. W., Jr. *J. Am. Chem. Soc.* **1989**, *111*, 9015.
(39) Wincel, H.; Mereand, E.; Castleman, A. W., Jr. *J. Phys. Chem.* **1994**, *98*, 8606.
(40) Harms, A. C.; Khanna, S. N.; Chen, B.; Castleman, A. W., Jr. *J. Chem. Phys.* **1994**, *100*, 3540.
(41) Armentrout, P. B. *Advances in Gas Phase Ion Chemistry*; Adams, N., Babcock, L. M., Eds.; Jai Press: Greenwich, CT, 1992; Vol. 1, pp 83−119.
(42) Dalleska, N. F.; Honma, K.; Armentrout, P. B. *J. Am. Chem. Soc.* **1993**, *115*, 12125.
(43) Dalleska, N. F.; Tjelta, B. L.; Armentrout, P. B. *J. Phys. Chem.* **1994**, *98*, 4191.
(44) Dalleska, N. F.; Honma, K.; Sunderlin, L. S.; Armentrout, P. B. *J. Am. Chem. Soc.* **1994**, *116*, 3519.
(45) Schultz, R. H.; Armentrout, P. B. *J. Phys. Chem.* **1994**, *98*, 4191.
(46) Lopez, X.; Ugalde, J. M.; Cossío, F. P.; Lecea, B.; Largo, A.; Barrientos, C. *J. Phys. Chem.* **1993**, *97*, 9337.
(47) Lopez, X.; Ugalde, J. M.; Cossío, F. P.; Lecea, B.; Largo, A.; Barrientos, C. *J. Phys. Chem.* **1994**, *98*, 3148.
(48) Lopez, X.; Irigoras, A.; Ugalde, J. M.; Cossío, F. P. *J. Am. Chem. Soc.* **1994**, *116*, 10670.
(49) Lopez, X.; Ugalde, J. M.; Cossío, F. P. *Can. J. Chem.* **1995**, submitted.
(50) Pearson, R. G. *J. Am. Chem. Soc.* **1963**, *85*, 3533.
(51) Pearson, R. G. *J. Chem. Educ.* **1965**, *581*, 643.
(52) (a) Pearson, R. G. In *Theoretical Models of Chemical Bonding*; Maksic, Z. B., Ed.; Springer-Verlag: Berlin, 1990; Part 1, pp 45−76. (b) Chattaraj, P. K.; Parr, R. G. In *Chemical Hardness*; Sen, K. D., Mingos, D. M. P., Eds.; Springer-Verlag: Berlin, 1993; Vol. 80, pp 11−25. (c) Chattaraj, P. K. *J. Ind. Chem. Soc.* **1992**, *69*, 173.
(53) Pople, J. A.; Head-Gordon, M.; Fox, D. J.; Raghavachari, K.; Curtiss, L. A. *J. Chem. Phys.* **1989**, *90*, 5622−5629.
(54) Curtiss, L. A.; Jones, C.; Trucks, G. W.; Raghavachari, K.; Pople, J. A. *J. Chem. Phys.* **1990**, *93*, 2537−2545.
(55) Curtiss, L. A.; Raghavachari, K.; Trucks, G. W.; Pople, J. A. *J. Chem. Phys.* **1991**, *94*, 7221−7230.
(56) (a) Parr, R. G.; Yang, W. *Density Functional Theory of Atoms and Molecules*; Clarendon Press: Oxford, U.K., 1989; p 278. (b) Becke, A. D. *J. Chem. Phys.* **1993**, *98*, 5648.
(57) Bader, R. F. W. *Atoms in Molecules. A Quantum Theory*; Clarendon Press: Oxford, U.K., 1990.
(58) Reed, A. E.; Curtiss, L. A.; Weinhold, F. *Chem. Rev.* **1988**, *88*, 899.
(59) For the basis set and method notations, see: Hehre, W. J.; Radom, L.; Schleyer, P. v. R.; Pople, J. A. *Ab-Initio Molecular Orbital Theory*; Wiley Interscience: New York, 1986 and references within.
(60) Scheiner, S. In *Reviews in Computational Chemistry*; Lipkowitz, K. B., Boyd, D. B., Eds.; VCH Publishers: New York, 1991; Vol. 2, p 165.
(61) Frisch, M. J.; Trucks, G. W.; Head-Gordon, M.; Gill, P. M. W.; Wong, M. W.; Forseman, J. B.; Johnson, B. G.; Schlegel, H. B.; Robb, M. A.; Repogle, E. S.; Gomperts, R.; Andres, J. L.; Raghavachari, K.; Binkley, J. S.; Gonzales, C.; Martin, R. L.; Fox, D. J.; Defrees, D. J.; Baker, J.; Stewart, J. J. P.; Pople, J. A. *Gaussian 92/DFT, Revision F.4*; Gaussian, Inc.: Pittsburgh, PA, 1992.

Table 1. Binding Energies and Relative Energies (in parentheses) (kcal/mol) Calculated at the G2 Level of Theory for Two-, Three-, and Four-Ligand Complexes

Two-Ligand Complexes

ligand	PL_2^+ (^3A)[a]	PL_2^+ (^3A)[a]	$PL^+\cdot L$ (^3A)	$PL^+\cdot L$(^1A)	$PXH_{n-1}\cdot XH_{n+1}^+$ (^1A)
NH_3	18.49(12.02)	55.10(0.00)	22.59(7.93)	no complex	21.57(0.30)
OH_2	19.56(7.82)	36.79(8.83)	27.37(0.00)	no complex	27.66(16.11)
FH	15.08(4.88)	18.23(26.55)	19.96(0.00)	20.39 (24.40)	

Three-Ligand Complexes

ligand	PL_3^+ (^3A)	PL_3^+ (^1A)	$PL_2^+\cdot L$ (^3A)	$PL_2^+\cdot L$(^1A)
NH_3	no complex	no complex	13.95 (11.04)	18.95 (0.00)
OH_2	no complex	12.71 (9.53)	18.10 (0.00)	20.53 (1.72)
FH	no complex	12.44 (26.28)	14.38 (0.00)	17.05 (21.67)

Four-Ligand Complexes

ligand	$P(L)_4^+$	ligand	$P(L)_4^+$
OH_2	no complex	FH	11.94

[a] Taken from ref 48.

2.2. Three- and Four-Ligand Complexes. Extensive searches for stationary points were carried out at the HF/6-31G(d,p) level of theory. When one such structure with all the frequencies positive was found, it was then reoptimized at the MP2/6-31G(d,p) level of theory. An additional MP2/6-31G(d,p) frequency calculation confirmed it to be a real minimum, for all force constants were positive.

G2 types of calculations are very costly for these complexes; however inclusion of a basis set similar to the largest one employed in G2 theory (i.e., the 6-311+G(3df,2p)) would be desirable to yield accurate binding energies. So, we decided to perform additional calculations within the framework of the density functional theory using the B3LYP functional.[56b] Hence, all structures were reoptimized at the B3LYP/6-31G(d,p) level of theory, and analytical frequencies at the stationary points were calculated at the B3LYP/6-31G(d,p) level of theory to confirm further that all of them were positive. The resulting structures are very similar to the MP2 ones, and both geometries can be found in Figures 2−4. At these geometries, single-point energy calculations with the 6-311+G(3df,2p) basis set were carried out. These energies were corrected for their corresponding ZPVE, evaluated at the B3LYP/6-31G(d,p) level of theory. They can be found in Table 2 of the supporting information. To carry out these calculations, we have used the GAUSSIAN92/DFT suite of programs.[61]

The total energies calculated in this way were employed to estimate the binding energies (D_0) of each of the clusters, according to eq 4, and they have been collected in Table 1 along with their relative energies. On the basis of our previous experience,[49] we think that the binding energies calculated in this way are accurate enough to compare with G2 ones, without significant errors that could affect the qualitative conclusions of this paper.

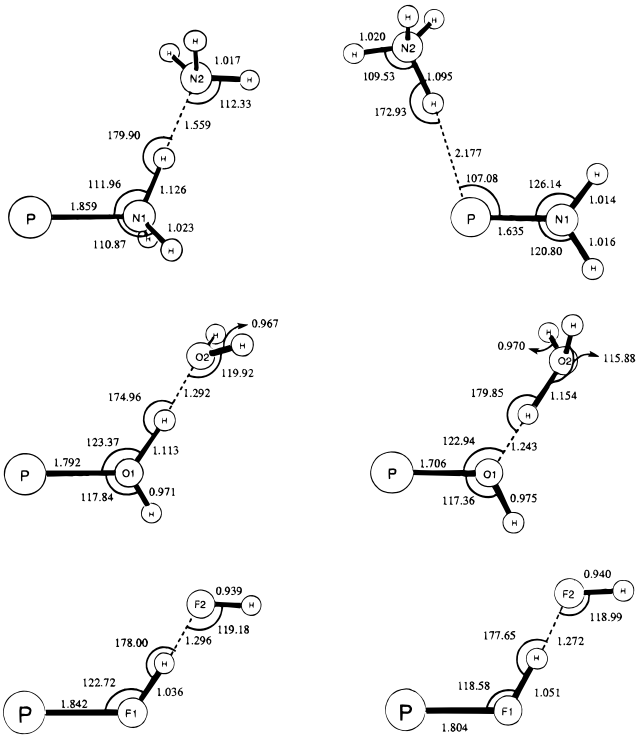

Figure 1. MP2/6-31G(d,p) geometries of the $PL^+\cdot L$ and $PXH_{n-1}\cdot XH_{n+1}^+$ complexes. Distances are in angstroms and angles in degrees. Triplets are on the left-hand side and singlets on the right-hand side.

2.3. Bonding Properties. For all complexes studied in the present paper, we have performed a Bader's topological analysis of $\rho(\mathbf{r})$ and $-\nabla^2\rho(\mathbf{r})$,[57] using the AIMPAC series of programs.[62] The MP2/6-311G(d,p)//MP2/6-31G(d) wave functions have been used to build up the electron density. Plots of their Laplacians are depicted in Figures 5−7. Properties of the bond critical points (r_c), such as $\rho(r_c)$ and $\nabla^2\rho(r_c)$, and the value of the energy density $H(r_c)$ are found in Table 3. The energy density at the bond critical point indicates a bond to be covalent if $H_{r_c} < 0$ and ionic if $H_{r_c} > 0$.[63] This criterion will serve us to discuss the degree of electronic stabilization in the binding mechanism.

The binding mechanism has been characterized further by means of the natural bond orbital (NBO) analysis,[58] and atomic charges have been estimated by means of the natural population

Table 2. Bonding Properties of the P−X and X−N Bonds for $PL^+\cdot L$ Complexes

Two-Shell Structures

		P−X_1			X_1−H			H−X_2		
Species		$\rho(r_c)$	$\nabla^2\rho(r_c)$	$H(r_c)$	$\rho(r_c)$	$\nabla^2\rho(r_c)$	$H(r_c)$	$\rho(r_c)$	$\nabla^2\rho(r_c)$	$H(r_c)$
$P(NH_3)^+\cdot NH_3$	^3A	0.1200	0.1051	−0.0940	0.2399	−1.0434	−0.3172	0.0800	0.0645	−0.0327
$P(OH_2)^+\cdot OH_2$	^3A	0.1088	0.2554	−0.0701	0.2097	−0.9409	−0.3204	0.1246	0.0226	−0.0837
$P(FH)^+\cdot FH$	^3A	0.0852	0.1418	−0.0493	0.2303	−1.3270	−0.4209	0.1031	0.1757	−0.0509
	^1A	0.0915	0.1928	−0.0535	0.2216	−1.2138	−0.3945	0.1111	0.1434	−0.0630

Proton Transfer Structures

		P−X_1			P−H			H−X_2		
$PNH_2\cdot NH_4^+$	^1A	$\rho(r_c)$	$\nabla^2\rho(r_c)$	$H(r_c)$	$\rho(r_c)$	$\nabla^2\rho(r_c)$	$H(r_c)$	$\rho(r_c)$	$\nabla^2\rho(r_c)$	$H(r_c)$
$PNH_2\cdot NH_4^+$	^1A	0.1684	0.7741	−0.1208	0.0426	0.0154	−0.0105	0.2640	−1.3046	−0.3769
		P−X_1			X_1−H			H−X_2		
$POH\cdot OH_3^+$	^1A	0.1269	0.5101	−0.0765	0.1450	−0.1285	−0.1235	0.1879	−0.6202	−0.2446

Table 3. Bonding Properties of the P−X and X−H Bonds for PL_2^+·L, PL_3^+, and $P(FH)_4^+$ Complexes

		X_2-P			$P-X_1$			X_1-H			$H-X_3$		
hydrogen bonded species		$\rho(r_c)$	$\nabla^2\rho(r_c)$	$H(r_c)$	$\rho(r_c)$	$\nabla^2\rho(r_c)$	$H(r_c)$	$\rho(r_c)$	$\nabla^2\rho(r_c)$	$H(r_c)$	$H(r_c)$	$\rho(r_c)$	$\nabla^2\rho(r_c)$
$P(NH_3)_3^+$·NH_3	^3A	0.0380	0.0729	−0.0035	0.0968	−0.0268	−0.0642	0.2861	−1.4297	−0.4253	0.0496	0.0955	−0.0100
	^1A	0.0993	0.0710	−0.0706	0.1122	0.1241	−0.0840	0.2693	−1.3427	−0.3892	0.0896	0.0399	−0.0175
$P(OH_2)_2^+$·OH_2	^3A	0.0371	0.1011	−0.0023	0.0891	0.0782	−0.0540	0.2741	−1.7954	−0.5190	0.0759	1.7054	−0.0237
	^1A	0.0813	0.0833	−0.0466	0.1042	0.2479	−0.0656	0.2617	−1.6507	−0.4857	0.0873	0.1588	−0.0335
$P(FH)^+$·FH	^3A	0.0354	0.1063	−0.0026	0.0719	0.0947	−0.0332	0.2673	−1.7821	−0.5273	0.0776	0.2254	−0.0218
	$^1A_1$	0.0622	0.0966	−0.0241	0.0815	0.1112	−0.0460	0.2546	−1.6243	−0.4897	0.0875	0.2193	−0.0308

		$P-X_1$			$P-X_2$			$P-X_3$		
phosphorus bonded species		$\rho(r_c)$	$\nabla^2\rho(r_c)$	$H(r_c)$	$\rho(r_c)$	$\nabla^2\rho(r_c)$	$H(r_c)$	$\rho(r_c)$	$\nabla^2\rho(r_c)$	$H(r_c)$
$P(OH_2)_3^+$	^1A	0.0867	0.1019	−0.0527	0.0687	0.0767	−0.0281	0.04411	0.0976	−0.0065
$P(FH)_3^+$	^1A	0.0634	0.0934	−0.0253	0.0486	0.1105	−0.0104	0.0486	0.1105	−0.0104
$P(FH)_4^+$	^1A	0.0486	0.1119	−0.0100	0.0420	0.1123	−0.0056			

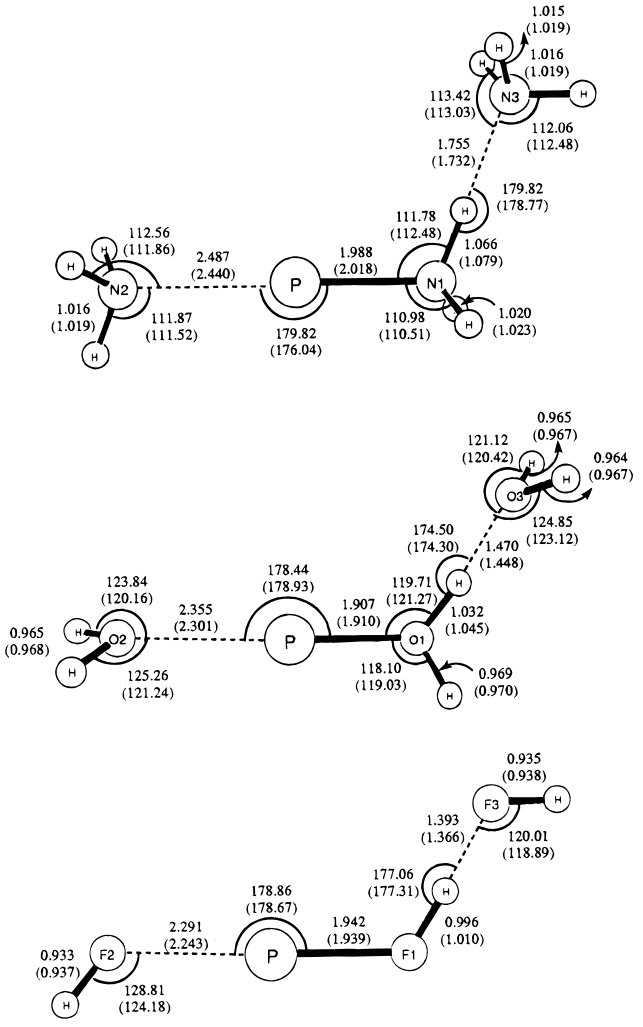

Figure 2. MP2/6-31G(d,p) and B3LYP/6-31G(d,p) (in parentheses) geometries of the triplet PL_2^+·L complexes. Distances are in angstroms and angles in degrees.

analysis (NPA). These results are summarized in Tables III−VI of the supporting information. Calculations were performed using the NBO code[64] as implemented in GAUSSIAN92/DFT.[61]

3. Results and Discussion

3.1. PL^+·L Complexes. As seen in Figure 1, remarkable differences have been found between triplet and singlet states for ammonia and water complexes. Namely, triplets maintain a two-shell structure during the optimization procedure, but singlets evolve to structures in which one proton is transferred from the inner to the outer ligand. We will call them proton transferred structures and refer to them as NH_4^+·PNH_2 and POH·OH_3^+ complexes. We will analyze their two spin states separately.

The hydrogen bond in triplet PL^+·L complexes is relatively strong. Thus, the $H-X_2$ bond distance is much shorter than for their corresponding ligand dimers[60] (R_{NN} is 3.15 Å for the ammonia dimer and R_{OO} is 2.910 Å for the water dimer at the MP2/6-31G(d,p) level of theory), and in addition, binding energies (Table 1) are also much larger (the largest binding energy for ligand dimers have been obtained for the water dimer, namely, −4.35 kcal/mol at the MP2/DZP level of theory, and including counterpoise correction,[65] experimental values[60] also lie between 4−5 kcal/mol). These surprisingly strong bonds cause these structures to lie even lower in energy than the corresponding triplet PL_2^+ structures (see relative energies in Table 1).

The shape of the Laplacian (Figure 5) and bonding properties such as $\rho(r_c)$ and $H(r_c)$ (Table 2) give some clues to the binding mechanisms. In the Bader's theory,[57,63] a regular hydrogen bond is described as a closed-shell interaction with a positive value of $H(r_c)$ and a low value of $\rho(r_c)$, which denotes the electrostatic character of the bond. However, in spite of the fact that the closed-shell shape of the Laplacian is maintained, a negative value of $H(r_c)$ and a relatively high $\rho(r_c)$ are encountered for the $H-X_2$ bonds of the PL^+·L complexes. This is indicative of a substantial sharing of the lone pair of the X_2 atom by the hydrogen of the inner ligand, which accounts for the strength of these bonds. This covalency was further confirmed by NBO analysis, which showed noticeable charge transfer interactions of the type $n_{X_2} \rightarrow \sigma^*_{X_1-H}$ (see Table IV of the supporting information).

The covalency of the $H-X_2$ bonds has a remarkable effect on the rest of the cluster. In comparing bonding properties of Table 2 with those reported[48] earlier for triplet PL^+ complexes (namely, the values of $\rho(r_c)$ and $H(r_c)$, in a.u., were found to be 0.1073 and −0.0808 for P−N, 0.0897 and −0.0553 for P−O, 0.0681 and −0.0307 for P−F; regarding hydride bonds, 0.3214 and −0.4689 for N−H, 0.3263 and −0.6477 for O−H, 0.3027 and −0.6339 for FH were found.), it can be assessed that some decreasing of the electron sharing (lower values of $\rho(r_c)$ and less negative values of $H(r_c)$) in X_1-H bonds and a concomitant enhancement of the covalency of $P-X_1$ bonds occurs. Thus, it seems that the covalency in $H-X_2$ bonds allows the X_1 atoms to withdraw electronic charge from X_1-H linking zones (this

(62) Biegler-Konig, F. W.; Bader, R. F. W.; Tang, T. H. *J. Comput. Chem.* **1980**, *27*, 1924.
(63) Cremer, D.; Kraka, E. *Croat. Chem. Acta* **1984**, *57*, 1259−1281.
(64) NBO Version 3.1, E. D. Glendening, A. E. Reed, J. E. Carpenter, and F. Weinhold.
(65) van Duijneveldt, F. B.; van Duijneveldt-van de Rijdt, J. G. C. M.; van Lenthe, J. H. *Chem. Rev.* **1994**, *94*, 1873.

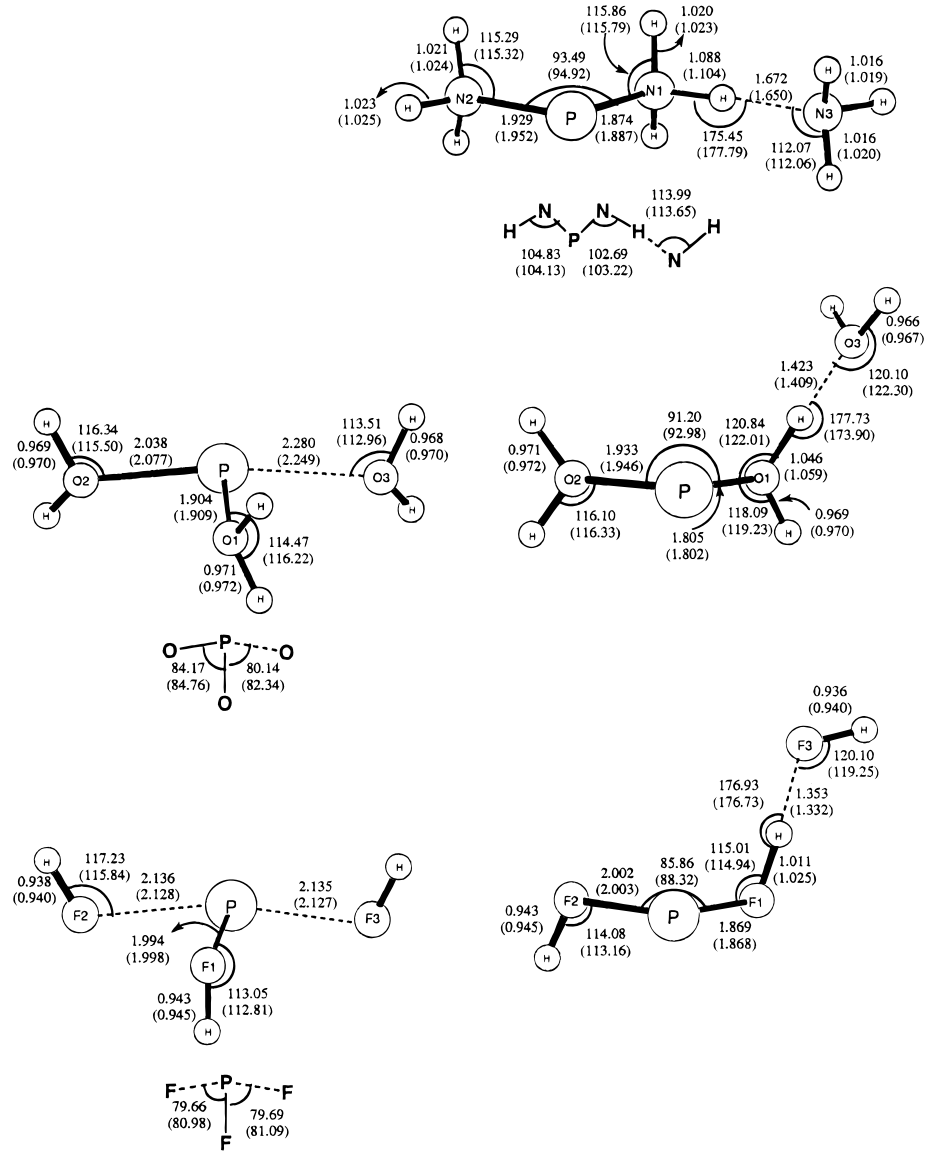

Figure 3. MP2/6-31G(d,p) and B3LYP/6-31G(d,p) (in parentheses) geometries for the singlet three-ligand complexes in both PL_3^+ and PL_2^+•L forms. Distances are in angstroms and angles in degrees.

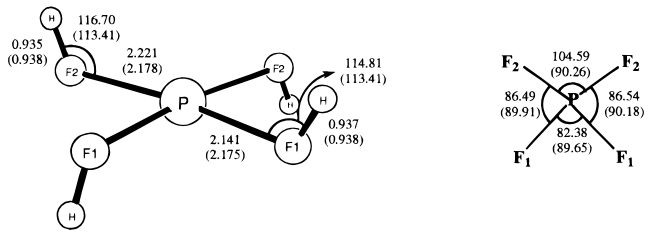

Figure 4. MP2/6-31G(d,p) and B3LYP/6-31G(d,p) (in parentheses) geometries for singlet $P(FH)_4^+$ complex. Distances are in angstroms and angles in degrees.

is particularly evident for the $P(FH)^+$•(FH) complex, for which electron charge deplexion zones connect F_1 and H atoms) and reinforces its donation to the P^+. The main structural consequences of this behavior are a significat shrinking of the P−X bonds and a lengthening of the X_1−H, when we add the outer ligand. In this sense, compare the P−X_1 bond distances of triplet PL^+•L complexes of Figure 1 with the previously reported data for triplet PL^+ complexes, namely, 1.030, 0.986, and 0.966 Å for N−H, O−H, and F−H bonds, respectively, and 1.915, 1.889, and 1.955 Å for P−N, P−O, and P−F bonds.

On the basis of these data, we can speak about a cooperative effect between the outer and inner ligands on the σ donation to the phosphorus ion. The final result is a reinforcement of the P−X bond due to the electronic charge transfer from the outer ligand. A concomitant partial transfer of the positive charge to the outer ligand occurs, and hence, sizeable positive charges ranging from 0.136 (FH) to 0.182 (OH_2) are encountered (Table III of the supporting information).

For the singlets, we found structures close to those reported for the triplets at the HF level. However, when electron correlation is included, the H−X_2 bond lengths shrink, and the H and X_2 basins are now bound by zones of electronic charge concentration, as is the case for normal hydride bonds[57] (see Figure 1 and the Laplacian of ρ in Figure 5). The removal of the proton by the outer ligand leads to an overall transfer of the positive charge to the newly formed NH_4^+ and OH_3^+ moieties, whose natural charge values are 0.735 and 0.814, respectively. Hence, the new complexes formed are better described as NH_4^+ and OH_3^+ ions bound to the PNH_2 and POH neutrals. In fact, the geometries for PNH_2 and POH moieties are very similar to those of the free neutrals,[66,67] for which remarkably short P−X bonds are found. Inspection of the values of the bonding properties along with the NBO analysis suggests a significant double-bond character for these bonds.

(66) Esseffar, M.; Luna, A.; Mó, O.; Yañez, M. *Chem. Phys. Lett.* **1993**, *209*, 557.

(67) Esseffar, M.; Luna, A.; Mó, O.; Yañez, M. *J. Phys. Chem.* **1993**, *97*, 6607.

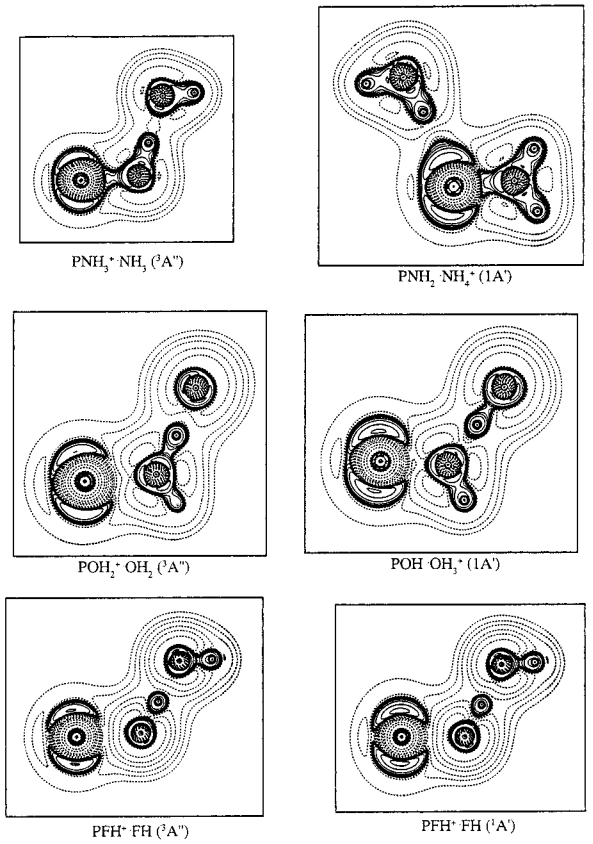

Figure 5. Contour maps of the $\nabla^2\rho$ of the $PL^+\cdot L$ and $PXH_{n-1}\cdot XH_{n+1}^+$ complexes. Negative values of $\nabla^2\rho$ are denoted by solid contours, positive values by dot contours. Remember that negative values of $\nabla^2\rho$ signify that the electron density ρ is locally concentrated in that zone of the space, whereas a positive value implies a local deplexion of charge. For all systems we have considered the plane which includes all the heavy atoms.

The cause of these proton transfers is the bigger electronic hole of the singlet P^+, since we have two formally empty 3p orbitals. This allows for a larger electron transfer, through π-type interactions, from the ligands. Ammonia exhibits one lone pair, which is already involved in a σ donation, so the partial π donation has to be accomplished by the electron pairs of the N−H bond. The presence of the outer ligand favors this process, providing the hydrogen with enough electronic charge to compensate for the loss in the X_1−H bond. When we are dealing with a soft ligand, for which the formation of a π bond is a very favored process,[48] the system just withdraws the pair of electrons involved in the X_1−H bond and forms a π bond with the phosphorus, releasing the proton to the outer ligand. Afterward, the NH_4^+ and the newly formed neutral are bound through a hydrogen bond. In the case of ammonia, NH_4^+ has to move around until it points to the lone pair of the phosphorus atom, since there is no lone pair associated with the N_1 basin. Water shows similarities with the ammonia case. However, the existence of two lone pairs in the water molecule allows for the OH_3^+ ion to remain bound to the O_1 atom. For both $NH_4^+\cdot PNH_2$ and $POH\cdot OH_3^+$ complexes, the new bonds are as strong as those of the triplet states, so comparable D_0's are predicted (see Table 1). Inspection of the Laplacian of ρ in Figure 5 and the bonding properties of Table 2 suggests that once again this noticeable bond strength is due to the significant covalency of the formal hydrogen bonds.

Finally, for the FH, the two-ligand shell structure is not lost when electron correlation is included. Undoubtly, although FH has properly oriented lone pairs, it is a too hard of a base to support strong π donation.

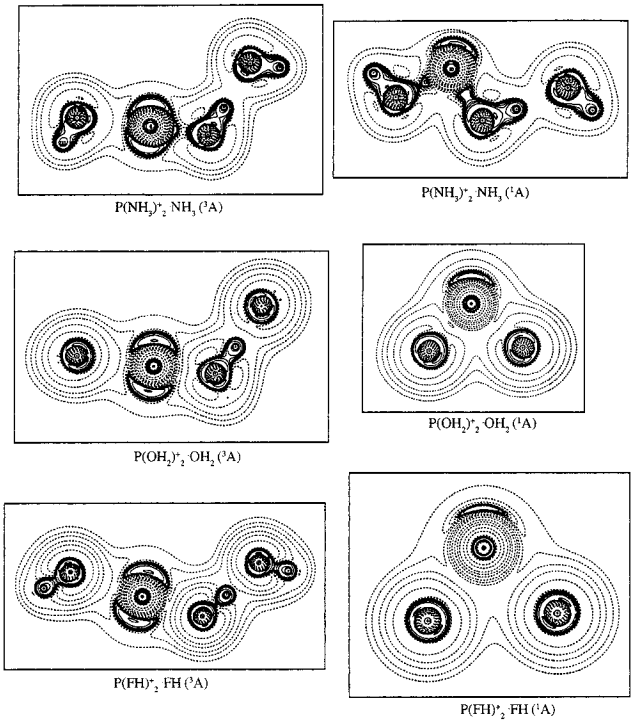

Figure 6. Contour maps of the $\nabla^2\rho$ of the triplet (left) and singlet (right) $PL_2^+\cdot L$ complexes. Negative values of $\nabla^2\rho$ are denoted by solid contours, positive values by dot contours. Remember that negative values of $\nabla^2\rho$ signify that the electron density ρ is locally concentrated in that zone of the space, whereas a positive value implies a local deplexion of charge. For triplet systems and the singlet ammonia complex, we have considered the plane which includes all of the heavy atoms. For singlet water and the FH complex, we have considered the plane formed by the phosphorus and the inner heavy atoms. The shape of the Laplacian for the hydrogen bond in the later systems is very similar to that observed for triplet complexes, and it has been omitted for the sake of brevity.

The processes described so far could have interesting chemical consequences. New chemical species could be formed if the second ligand adds on the H position in singlet one-ligand complexes. Singlet PNH_2 and POH species could be formed with the release of NH_4^+ and OH_3^+ ions, respectively. The relative energies of the two ligand species are reported in Table 1. In the water case, the $POH\cdot OH_3^+$ complex is the highest in energy, whereas for ammonia, the $NH_4^+\cdot PNH_2$ complex is almost degenerate with the lowest-energy isomer, namely, $P(NH_3)_2^+$ (^{1}A). Therefore, we suggest that ammonia clusters are more likely to undergo conversion reactions than water clusters.

3.2. Three-Ligand Complexes. Two types of three-ligand complexes have been considered: those with the third ligand added on the phosphorus (PL_3^+ complexes) or on one of the hydrogens of the inner shell ($PL_2^+\cdot L$ complexes). For triplets all the attempts to optimize structures of the PL_3^+ type failed. The new ligand migrates until it binds a hydrogen of one of the inner ligands. This behavior can be understood by looking at the Laplacian of ρ of the triplet $PL_2^+\cdot L$ complexes (see Figure 6). Zones of electronic charge concentration surround the phosphorus basin in all directions, except for the one in which the two inner ligands are bound. Hence, it is clear that further approach of another ligand pointing to the P^+ would be highly unfavored because of the Pauli repulsion between the lone pairs of the ligand and the valence shell of the phosphorus.

Regarding the singlet states, we have been able to characterize the PL_3^+ type of complexes for water and FH, whereas in the case of the ammonia complex, as found for the triplets, the third

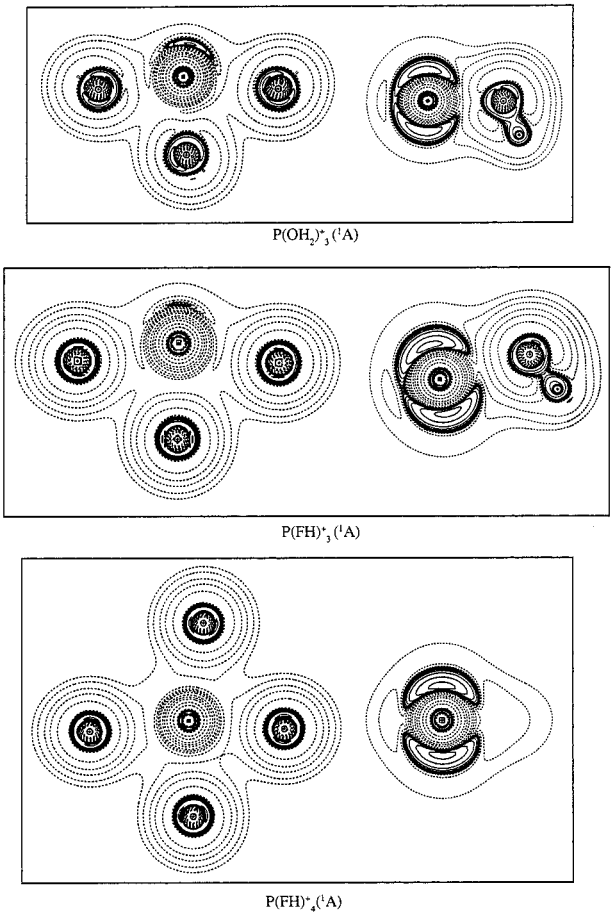

Figure 7. Contour maps of the $\nabla^2\rho$ of the PL_3^+ complexes. Negative values of $\nabla^2\rho$ are denoted by solid contours, positive values by dot contours. Remember that negative values of $\nabla^2\rho$ signify that the electron density ρ is locally concentrated in that zone of the space, whereas a positive value implies a local deplexion of charge. For triplet systems and the singlet ammonia complex, we have considered the plane which includes all of the heavy atoms. Two planes are considered for each system.

ligand migrates to bind one of the inner ligands. We will now comment upon the PL_2^+·L and PL_3^+ cases in turn.

3.2.1. (PL_2^+)L Complexes. The inner ligands in these complexes adopt similar conformations to the those observed for PL_2^+ complexes.[48] The outer ligand is bound through a hydrogen bond of similar characteristics to that described for the PL^+·L complexes, but with a less pronounced covalency (compare values of $H(r_c)$ across Tables II and III), and hence, larger $H-X_3$ distances and lower binding energies are obtained for them. The formation of the hydrogen bond has similar cooperative effects on the first ligation shell as for the PL^+·L complexes, but less developed, in agreement with the lower covalency of the outer−inner ligand bonds.

On the other hand, in the case of triplets, their large $P-X_2$ bond distances and near-zero value of their $H(r_c)$ are suggestive of a predominantly electrostatic bonding for the second inner ligand. This contrasts with the behavior of singlets, for which a sizeable covalency is still kept. These differences can be easily understood by taking into account that there is only one empty 3p orbital in the triplet P^+. When one of the inner ligands enhances its donation to the 3p orbital, the other inner ligand has to minimize it accordingly. However, in the singlets, two empty 3p orbitals of the phosphorus coexists, and each interacts with a different ligand. Therefore, the enhanced donation ability of one ligand has not such a large effect on the donation of the other.

3.2.2. (PL_3^+) Complexes. As it can be readily appreciated from Figure 3, these complexes show a T-like structure. This behavior poses a distinction with respect to other ions of the same row such as Na^+ or Mg^+, for which C_3 planar and pyramidal structures have been reported.[7,11,21] As can be observed in the plots of $\nabla^2\rho(r)$ (Figure 7), the *T*-like structures enable the valence electronic charge of the P^+ to polarize away from the ligand bonding directions, so it minimizes the repulsion between the lone pairs of the ligands and the valence electrons of P^+. This effect, along with the reported natural charges for singlet two-ligand complexes,[48] could shed some light on the reason for the nonexistence of ammonia complexes of the PL_3^+ type. For the singlet $P(NH_3)_2^+$ complex,[48] the charge on the phosphorus (Q_P) is only +0.348 due to the large covalency of the P−N bonds; this charge is even smaller than that exhibited by the hydrogens (Q_H), i.e. +0.434. For the T geometry, the new ligand approaches one of the hydrogen of the other ligands. If this hydrogen has a sensibly larger positive charge than the phosphorus (as it is for the ammonia case), it should be expected that ammonia will bind to the hydrogen instead to the phosphorus. However, when the covalency of the P−X bonds in singlet two-ligand complexes is lower, the phosphorus retains a larger positive charge.[48] It turns out that for OH_2 ($Q_P = 0.526$; $Q_H = 0.543$) and *FH* ($Q_P = 0.625$; $Q_H = 0.620$) this is high enough to get the new ligand bound to the phosphorus.

Both PL_3^+ complexes show similar binding energies, which are lower than those of singlet two-ligand complexes PL_2^+, (−36.79 kcal/mol for OH_2 and −18.23 for FH). It is worth noting that PL_3^+ complexes are less stable than the corresponding PL_2^+·L complexes (see relative energies in Table 1).

3.3. Four-Ligand Complexes. We have tried to add a fourth ligand to the P^+ ion in PL_3^+ complexes. At the HF level of theory, all attempts to optimize a $P(OH_2)_4^+$ complex failed. However, we have characterized a $P(FH)_4^+$ complex (Figure 4).

Quite interestingly, at the MP2/6-31G(d,p) level of theory, we have obtained a $P(FH)_4^+$ complex with two different P−X bonds. Two FH are bound to phosphorus at 2.141 Å, while the two others are bound at a larger distance of 2.221 Å. The Laplacian shows a situation in which the valence shell of charge concentration of the phosphorus atom is totally concentrated out of the plane of the F atoms, and the ligands are located in the electronic charge deplexion plane (see Figure 7). Remarkably, at the B3LYP/6-31G(d,p) level of theory, the differences between the $P-F_1$ and $P-F_2$ bonds are lowered to a large extent. Now we obtain four similar P−F bonds with a bond distance lying between the two of the MP2 method. The binding energy of the fourth, 11.94 kcal/mol, is only slightly lower than that of the third ligand in the $P(FH)_3^+$ complex.

4. Concluding Remarks

Within this and previous papers, we have dealt with 40 clusters of phosphorus positive ion with first- and second-row hydrides in both their singlet and triplet states. Highly accurate ab-initio techniques have been employed to determine their geometries and stabilities. Besides, a rigorous analysis of the total electron density has also been carried out, in order to gain insight on the binding mechanisms. In this section we will state some of the general features or rules satisfied by P^+ clusters of PL_n^+ and PL_{n-1}^+·L types. For this purpose it is useful to have a look at Figure 8, in which the D_0's and the values of $H(r_c)$ for P−X bonds (a measure of the covalency) for PL_n^+ (n = 1−4) complexes are summarized. In our opinion, P^+ is a good case of study of the behavior of soft ions, and therefore, the following conclusions could also be useful for the understanding of clusters of other soft ions.

(1) In one-ligand (^{3}P)P^+ clusters, and one- and two-ligand (^{1}D)P^+ clusters, the phosphorus cation behaves as a soft acid.

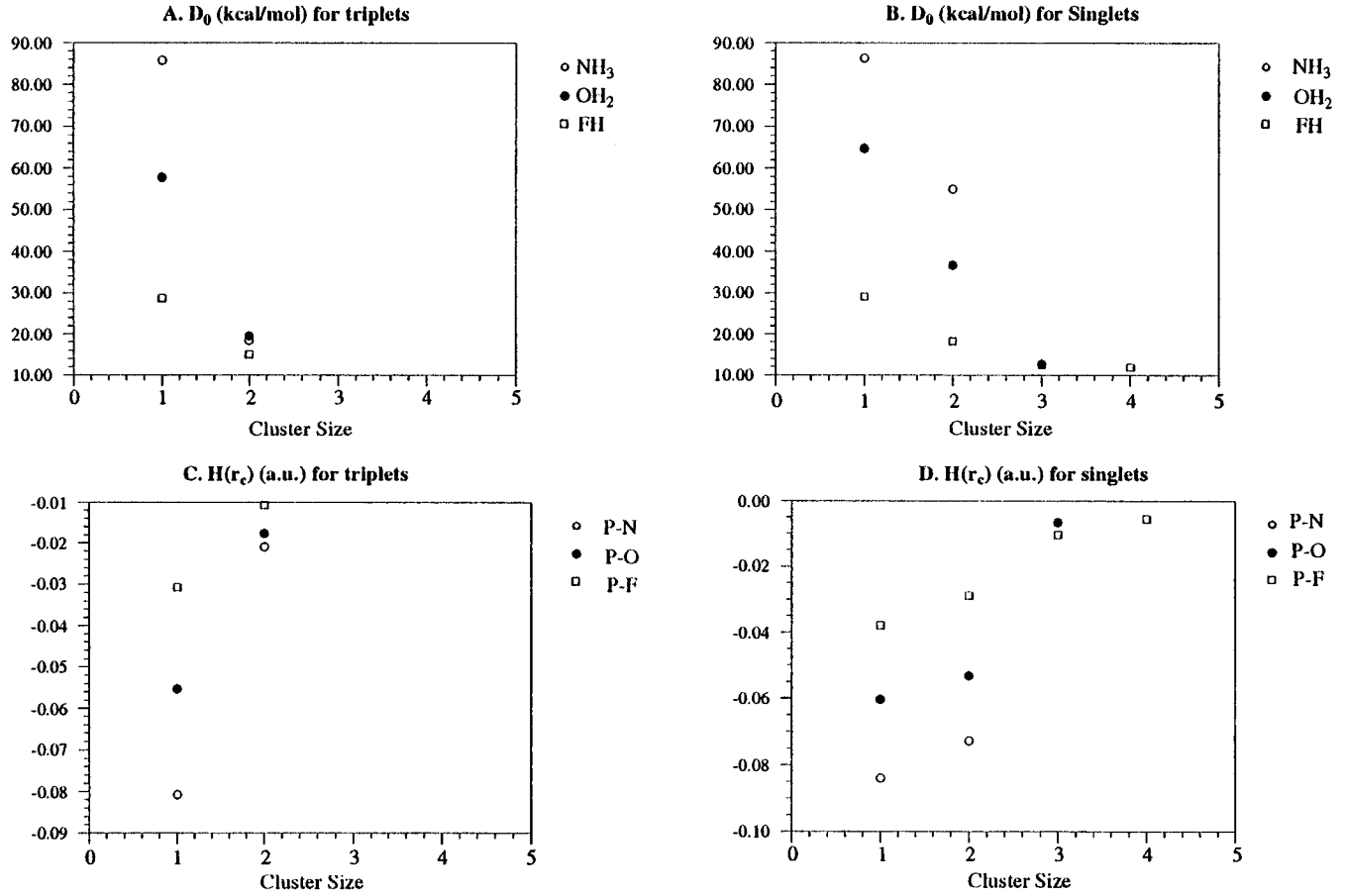

Figure 8. Plots showing the decrease in binding energies for triplet (A) and singlet (B) PL_n^+ ion−molecule complexes (L = NH_3, OH_2, FH; n = 1, 4). In the bottom diagrams, the values of $H(r_c)$ for the P−X bonds are given for both triplet (C) and singlet systems (D). We recall that this magnitude can be considered as a measure of the covalency of the P−X bonds. Notice that the sharp decrease in binding energies matches the large decrease in the covalency. Also, the type of decrease (smooth or sharp) in binding energies fits the behavior in $H(r_c)$.

Therefore, according to the HSAB principle, it forms stronger bonds with the softest bases for which electronic interactions are favored.

(2) Successive binding energies decrease smoothly and drop suddenly for $n = 2$ for $(^3P)P^+$ and $n = 3$ for $(^1D)P^+$, respectively, which correspond to the saturation of the valence electronic shell of the central ion.

(3) Soft ligands show sharp binding energy decreases, whereas hard ligands show smooth ones. This is a consequence of the different degree of covalency of the P−X bonds. The more electrostatic the P−X bond, the smoother the lowering is.

(4) The maximum number of ligands in the first solvation shell is $n = 2$ for triplets, whereas for singlets, it is $n = 2$ for ammonia, $n = 3$ for water, and $n = 4$ for FH. The behavior of the triplets is related with the repulsion originated by the unpaired electrons of the phosphorus cation, whereas in the singlets, it is related to the covalency of the P−X bonds. The larger the covalency, the larger the decline of the positive charge of the phosphorus, therefore the smaller the number of ligands that can bound to it.

(5) The second ligation shell has a significant effect on the backbone of the first one, namely, it reinforces the P−X bond. The hydrogen bonds between the two ligand shells show a significant covalency, allowing for larger electron donation to the phosphorus ion and confering to the cluster with a larger stability.

(6) Thermodynamically favored structures for phosphorus ion clusters are those that maximize the amount of electronic charge donated to the phosphorus ion. This does not necessarily imply direct bonding between the ligand and phosphorus ion, since it can be more efficient by bonding on the second ligation shell, through cooperative effects.

(7) Conversion processes are possible for singlet $PL^+{\cdot}L$ types of complexes of ammonia and water. This involves formation of PNH_2 and POH neutrals bound to ammonium and hydronium ions, respectively. The P−X bonds for these neutrals exhibit a substantial double-bond character.

Acknowledgment. This research has been supported by the Spanish Office of Science and Education (Ministerio de Educacion y Ciencia) Grant No. PB91-0456 and the Basque Provintial Government of Guipuzcoa (Gipuzkoako Foru Aldundia). X.L. thanks the Basque Government (Eusko Jaurlaritza) for a grant.

Supporting Information Available: Tables of MP4/6-311G(d,p), total energies, and natural changes of the phosphorus and ligands of $PL^+{\cdot}L$ and $PL_2^+{\cdot}L$ as well as a summary of the natural bond orbital analyses (6 pages). This material is contained in many libraries on microfiche, immediately follows this article in the microfilm version of the journal, can be ordered from the ACS, and can be downloaded from the Internet; see any current masthead page for ordering information and Internet access instructions.

JA952257G